Journal of Power Sources 257 (2014) 272–279

Contents lists available at ScienceDirect

Journal of Power Sources

journal homepage: www.elsevier.com/locate/jpowsour

Gold electrode modified with a self-assembled glucose oxidase and 2,6-pyridinedicarboxylic acid as novel glucose bioanode for biofuel cells

Malika Ammam [a,b,*], Jan Fransaer [b]

[a] Faculty of Mathematics and Natural Sciences, Products and Processes for Biotechnology – Institute for Technology, Engineering & Management, University of Groningen, Nijenborgh 4, 9747 AG Groningen, The Netherlands
[b] Department of Metallurgy and Materials Engineering (MTM), K.U. Leuven, Kasteelpark Arenberg 44, B-3001 Heverlee, Belgium

HIGHLIGHTS

- 2,6-Pyridinedicarboxylic acid is a useful electron mediator for glucose oxidase.
- 2,6-Pyridinedicarboxylic acid and glucose oxidase were assembled on gold electrode.
- In presence of the mediator, glucose oxidation occur 461 mV earlier.
- The non-compartmentalized biofuel cell generated a power output of 25 μW mm^{-2}.

ARTICLE INFO

Article history:
Received 18 November 2013
Received in revised form
30 January 2014
Accepted 3 February 2014
Available online 12 February 2014

Keywords:
Glucose oxidase
Self-assembled enzyme layers
Glucose bioanode
Biofuel cells

ABSTRACT

In this study, we have constructed a gold electrode modified with (3-aminopropyl)trimethoxysilane/2,6-pyridinedicarboxylic acid/glucose oxidase (abbreviated as, Au/ATS/PDA/GOx) by sequential chemical adsorption. Au/ATS/PDA/GOx electrode was characterized by Fourier Transform Infrared Spectroscopy (FT-IR) and Electrochemical Impedance Spectroscopy (EIS). The data from FT-IR illustrated deposition of ATS, PDA and GOx on the surface of gold electrode. The latter has been confirmed by EIS which showed that the electron transfer resistance of the electrode increases after adsorption of each supplementary layer. Linear sweep voltammetry (LSV) in phosphate buffer solution containing 5 mM glucose displayed that compared to Au/ATS/GOx, oxidation of glucose at Au/ATS/PDA/GOx electrode starts 461 mV earlier. This gain in potential is attributed to presence of PDA in the constructed Au/ATS/PDA/GOx electrode, which plays some sort of electron mediator for glucose oxidation. The Au/ATS/PDA/GOx electrode was stabilized by an outer layer of polystyrene sulfonate (PSS) and was connected to a Pt electrode as cathode and the non-compartmentalized cell was studied under air in phosphate buffer solution pH 7.4 containing 10 mM glucose. Under these conditions, the maximum power density reaches 0.25 μW mm^{-2} (25 μW cm^{-2}) for the deposited GOx layer that has an estimated surface coverage of ~70% of a monolayer.

1. Introduction

Enzyme-based biofuel cells (BFCs) utilize enzymes to catalyze chemical reactions, thus replacing traditional expensive metal electrocatalysts such as platinum employed in conventional fuel cells. Furthermore, by contrast to fuel cells where strong or harsh conditions maybe required for cell operation, enzyme biofuel cells generate electricity under mild conditions through the oxidation of renewable energy sources without greenhouse gas emissions or environmental pollution. In that respect, enzyme biofuel cells employ near-room temperature and neutral pH operation [1], which make them not only useful for biomass conversion but also as potential alternative power sources for *in vivo* applications for implantable biomedical devices like miniaturized sensors transmitters and artificial organs. To date, the vast majority of enzyme biofuel cells are based on the electroenzymatic oxidation of glucose

* Corresponding author. Faculty of Mathematics and Natural Sciences, Products and Processes for Biotechnology – Institute for Technology, Engineering & Management, University of Groningen, Nijenborgh 4, 9747 AG Groningen, The Netherlands. Tel.: +31 503639237; fax: +31 503632990.
E-mail addresses: m78ammam@yahoo.fr, m.ammam@rug.nl (M. Ammam).

http://dx.doi.org/10.1016/j.jpowsour.2014.02.007
0378-7753/

at the bioanode and oxygen reduction at the biocathode. However, assembly of enzymes on the electrode surfaces usually does not achieve significant electron transfer between the immobilized enzymes and the current collector or the electrode, mostly because of the electrical insulation of the active sites of the enzyme by the surrounding protein shells [2]. To overcome the problem, electron mediators are introduced to shuttle electrons between the active sites of the enzyme and the electrode surface [3].

Judicious choice of the electron mediator at enzyme bioanodes and biocathodes is essential to maximize BFC power output. Desirable characteristics for electron mediators include: rapid heterogeneous, enzyme-mediator and self-exchange electron transfer rates, for delivery of electrons; and chemical stability in oxidized and reduced forms, to ensure stability of catalytic turnover of enzyme reaction. To date, a large number of electron mediators have been investigated for enzyme biofuel cells with variable degrees of success [4–14]. In this paper, we introduce 2,6-pyridinedicarboxylic acid as a useful electron mediator for glucose oxidase modified gold electrode. The enzyme electrode exhibited reasonable current response and low starting potential of glucose oxidation, promising to be optimized and used as an efficient bioanode in glucose/O_2 biofuel cells.

2. Experimental

2.1. Materials

Ultrapure water milliQ grade with a resistivity of 18.2 MΩ cm was used for all the experiments. Glucose oxidase (GOx) crude from *Aspergillus Niger* (211 units mg^{-1}) was purchased from Sigma–Aldrich. Glucose (Glu) was purchased from Acros Organic and the glucose solution was prepared 24 h before use. H_2O_2 60% and H_2SO_4 90% from Acros Organic or Fisher. (3-Aminopropyl)trimethoxysilane 97% (ATS), 2,6-pyridinedicarboxylic acid 99% (PDA) and sodium polystyrene sulfonate (PSS) were from sigma. Phosphate salts (NaH_2PO_4 and Na_2HPO_4) and sodium chloride analytical grade were purchased from Acros Organic. The buffered saline pH 7.4, used for the testing of the GOx electrodes, was prepared from phosphate salts (0.1 M) and sodium chloride (0.15 M). Gold (Au) electrode rode 1 mm in diameter (surface area 0.78 mm^2) is used as a substrate for deposition and working electrode and was purchased from Goodfellow.

2.2. Equipment and procedures

Spectrum 100 FT-IR from Perkin Elmer was used for the Fourier Transform Infrared Spectroscopy (FT-IR) studies. A potentiostat from Solartron Instruments model SI 1287 was used for testing the enzymes electrodes using Linear Sweep Voltammetry (LSV). A three compartment electrochemical cell was used. The side arms contained an Ag/AgCl wire as reference electrode and a platinum counter electrode with surface area of 1 cm^2. The distance between the gold working electrode and the counter electrode is about 1.5 cm. Measurements were made at room temperature in 5 mL phosphate buffer solution pH 7.4. The gold electrode either before or after modification was polarized between −0.4 V and +0.5 for each LSV. For the Electrochemical Impedance Spectroscopy (EIS) measurements, the potentiostat was used in combination with an SI 1255 HF frequency response analyzer. Voltage and current measurements of the BFCs were carried out with two multimeters from Fluke 87 True RMS. The BFCs current and voltage were varied using a potentiometer (1 MΩ). The units of power density are expressed in μW mm^{-2} because the final goal of these electrodes is to power miniaturized electronic devices for *in vivo* application of which small surface area electrodes are usually employed.

2.3. Preparation of the Au/ATS/PDA/GOx electrode

First, the clean and dried Au electrode under Nitrogen flow was treated with piranha solution (mixture of 90% H_2SO_4 + 60% H_2O_2 at proportion of 3:1 by volume) at a temperature above 90 °C for about 1 h. The electrode was then abundantly cleaned with ultrapure water and dried under nitrogen flow. This step allows a deep cleaning of the Au electrode and may also result in formation of thin layer of gold oxides on top of the gold electrode [15–17]. The clean oxidized and dried Au electrode was then treated with pure ATS by immersing the electrode in ATS solution for at least 15 min. The electrode was then removed, rinsed with ultrapure water and dried under nitrogen flow. Although at this stage it is not clear what happened during this step, our results indicate deposition of a layer of ATS on the gold electrode. On the other hand, presence of amine groups in ATS makes probably the electrode positively charged (Fig. 1) [18–22]. Other scenarios where for example the amino group of aminopropyltrimethoxysilane are adsorbed on hydroxylated surfaces prior to silylation are also possible. Afterward, the Au/ATS electrode was then immersed in 1 mL ultrapure water containing 5 mg PDA for at least 15 min. PDA is chemically adsorbed on ATS via probably electrostatic interactions (Fig. 1). This layer was found to be very important for mediation of glucose oxidation, perhaps due to the aromatic ring in PDA. Afterward, the Au/ATS/PDA was immersed in GOx solution containing 50 mg mL^{-1} ultrapure water for at least 15 min. Though it is not yet clear how PDA is linked to GOx, our results demonstrate that both entities are close enough to communicate and yield better electron transfer. It is worth noting that similar behaviors have been observed elsewhere between pyridines or similar rings and proteins or enzymes [4,22–26]. Finally, the electrode was rinsed gently with ultrapure water and dried. The preparation of the other electrodes used for comparison such as Au/ATS/GOx followed similar process. In other words, the electrode was dipped in same solutions of (ATS, GOx) for 15 min then removed, gently cleaned with ultrapure water and dried.

3. Results and discussion

3.1. Characterization of Au/ATS/PDA/GOx electrode

Fig. 2 displays FT-IR spectra of Au electrode after modification with ATS (a), ATS/PDA (b) and ATS/PDA/GOx (c). All spectra have been taken with subtracted backgrounds. The chemical adsorption and polymerization of the silane ATS on the Au electrode is visible in the regions of 3521–2607 cm^{-1}, 1594–1275 cm^{-1} and 1107–823 cm^{-1} (Fig. 2a). The bands located at 1102 cm^{-1}, 1020 cm^{-1} and 956 cm^{-1} are assigned to the SiO–H and Si–O–Si groups [18]. The absorption bands at 907 cm^{-1} and 837 cm^{-1} revealed the presence of Si–O–H stretching and OH vibrations on the surface of Au. The two broad bands at 3352 cm^{-1} and 1660 cm^{-1} can be ascribed to the N–H stretching vibration and NH_2 bending mode of free NH_2 group, respectively [27,28]. In addition, hydrogen-bonded silanols also absorb at around 3200 cm^{-1} and 3470 cm^{-1} [27,29]. The presence of the anchored propyl group was confirmed by C–H stretching vibrations that appeared at 2935 cm^{-1} and 2839 cm^{-1}. On the other hand, as shown in Fig. 2b, chemical adsorption of PDA on the Au/ATS electrode can mainly be distinguished in the region of 1777–1252 cm^{-1}, where supplementary enhanced bands appear. The latter will be assigned to presence of additional carboxylic and amine groups from the pyridine ring [30]. A zoom and comparison between the FT-IR spectra of ATS, PDA and ATS/PDA in the frequency range of 1800–1200 cm^{-1} is depicted in Fig. 3 and for comparison, the main transmission bonds of each of ATS, PDA and ATS/PDA are mentioned in caption of Fig. 3. If covalent binding

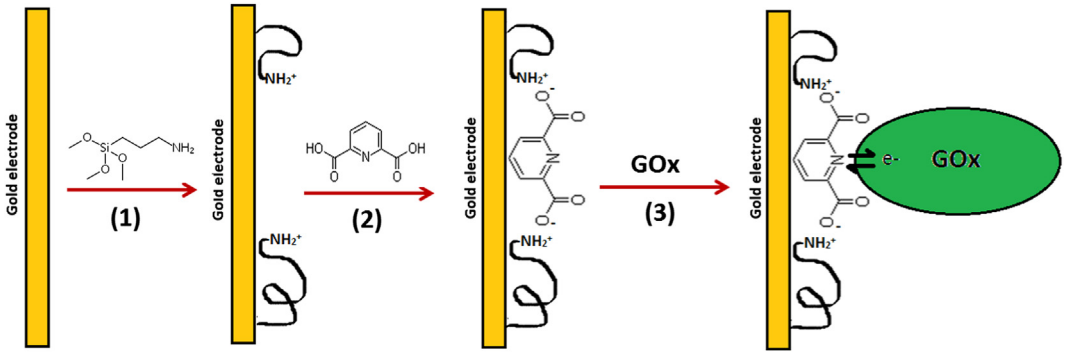

Fig. 1. Schematic representation of one of the plausible scenarios of the gold electrode after modification with (3-aminopropyl)trimethoxysilane (1), 2,6-pyridinedicarboxylic acid (2), glucose oxidase (3) to form a self-assembled film Au/ATS/PDA/GOx.

between ATS and PDA occurs, it may happen through two possible ways: i) binding of the oxygen of PDA to the nitrogen of ATS to form an O–N bond or, ii) binding of the carbon of PDA to the nitrogen of ATS to form an amide function. Analysis of the spectrum of ATS/PDA in the region of 1680–1630 cm^{-1} revealed no particular bond in that region to suggest an amide formation (Fig. 3). Similarly, N–O bond is characterized by a strong absorption band in the region of 1560–1515 cm^{-1} and a double absorption band in the frequency region of 1385–1345 cm^{-1} [30]. The ATS/PDA spectra of Fig. 3 shows neither a strong bond in the region of 1560–1515 cm^{-1} or a double band at 1385–1315 cm^{-1} to suggest presence of covalent bonding between the oxygen of PDA and nitrogen of ATS. Fig. 3 reveals that spectrum of ATS/PDA is simply the sum of spectra of ATS and PDA. This strongly suggests that interaction between both components is based on electrostatic rather than covalent binding. As depicted in Fig. 2c, addition of GOx to the film enhances particularly the bands at 1762–1299 cm^{-1}. This was expected since GOx is mainly characterized by the spectral features at 1658 cm^{-1} assigned to C=O stretching from amide I and 1548 cm^{-1} assigned to NH deformation in amide II [31].

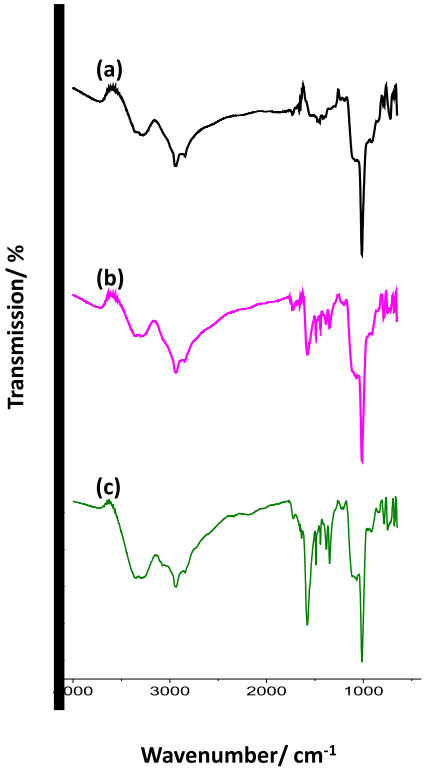

Fig. 2. FT-IR spectra of Au/ATS (a), Au/ATS/PDA (b) and Au/ATS/PDA/GOx (c). For all spectra a, b and c, the background of the unmodified Au substrate was subtracted.

In order to gain a better understanding of the chemical assembly, Au/ATS/PDA/GOx electrode was further characterized by EIS. Fig. 4 depicts EIS measurement shown as Nyquist plots of unmodified Au electrode, Au/ATS and Au/ATS/PDA/GOx. In a typical Nyquist plot, the semicircle part at higher frequencies correspond to the electron transfer limited process and the diameter of the semicircle is equivalent to the electron transfer resistance (R_{et}), which controls the electron transfer kinetics of the redox probe at the electrode interface and, the linear part at lower frequencies correspond to the diffusion process [32]. Hence, the complex impedance data can be modeled by Warburg impedance (Z_w) schematically displayed in the inset of Fig. 4A. Some of the completed semicircles (by drawing) are highlighted in solid green lines in Fig. 4B. Fig. 4B clearly displays a gradual increase in the semicircle after deposition of each supplementary layer. This means that the electron transfer resistance, R_{et}, increases after deposition of each supplementary component. The Eq. (1) may explain the relationship between the current due to $K_4[Fe(CN)_6]/K_3[Fe(CN)_6]$ that flows through the deposited film and the electron transfer resistance [33]:

$$R_{et} = RT/nFi \quad (1)$$

where R is the ideal gas constant, T is the absolute temperature, n is the number of transferred electrons per one molecule of the redox probe, F is faraday constant and i is the exchange current. Since R, T,

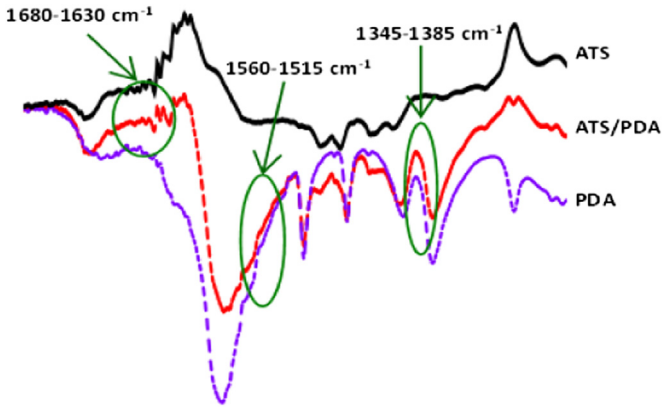

Fig. 3. Comparison between FT-IR spectra of ATS, PDA and ATS/PDA in the frequency range of 1800–1200 cm^{-1}. The main transmission bonds of ATS, PDA and ATS/PDA are below: *ATS*: 1730, 1655, 1647, 1638, 1596, 1545, 1471, 1450, 1415, 1391, 1337, 1289, 1229 cm^{-1}. *PDA*: 1730, 1714, 1635, 1580, 1548, 1490, 1442, 1380, 1348, 1257, 1215, 1203 cm^{-1}. *ATS/PDA*: 1733, 1727, 1654, 1648, 1638, 1578, 1547, 1491, 1471, 1456, 1442, 1418, 1383, 1347, 1289, 1259, 1229, 1216, 1203 cm^{-1}.

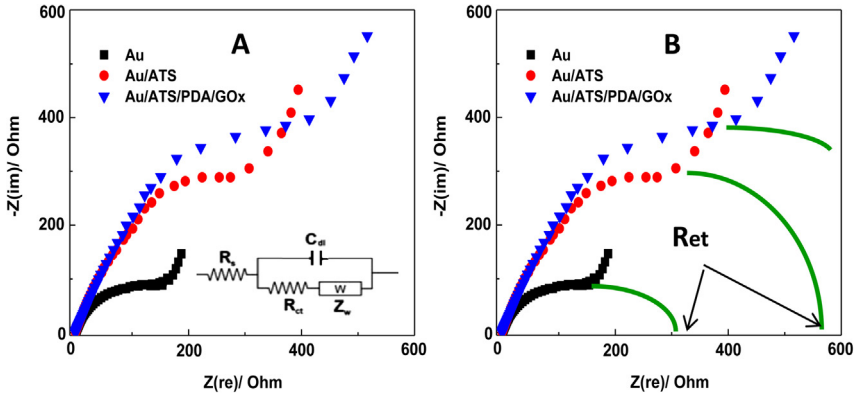

Fig. 4. (A) Nyquist plots (Z(im) versus Z(re)) of Au electrode, Au/ATS, and Au/ATS/PDA/GOx. Inset of A represents the electrical equivalent circuit at interface electrode/electrolyte (Randles circuit); R_s is the electrolyte resistance; R_{et} is the charge transfer resistance; Z_w is the so-called the Warburg impedance and, C_{dl} is the electrochemical double layer capacity. (B) is (A) by completing the semicircles (solid green lines) showing R_{et} for Au and Au/ATS electrodes. For Au/ATS/PDA/GOx, R_{et} is higher and located outside the scale window. Testing conditions: 5 mM $K_4[Fe(CN)_6]/K_3[Fe(CN)_6]$ (1:1) in buffered saline pH 7.4 prepared from phosphates salts (0.1 M) and sodium chloride (0.15 M), frequency range between 0.1 and 100,000 Hz, open circuit potential. (For interpretation of the references to colour in this figure legend, the reader is referred to the web version of this article.)

F and n are constants for all the electrodes, an increase in R_{et} indicates a decrease in i. This means that the insulating properties of the electrode increase respectively after deposition of ATS and ATS/PDA/GOx due to the increase in film thickness. However, it is worth noting that because the deposited film is thin, it increases only by few hundred of ohm. These observations suggest that all components, ATS, PDA and GOx are well immobilized on the Au electrode.

3.2. Glucose electrooxidation at Au/ATS/PDA/GOx electrodes

Fig. 5A shows the electrochemical response of unmodified Au electrode without and with 5 mM glucose and Au/ATS/PDA/GOx modified electrode without and with 5 mM glucose. As expected Au electrode does not catalyze the oxidation of glucose because same LSV is obtained before and after addition of 5 mM glucose. On the other hand, compared to the response of Au/ATS/PDA/GOx without presence of glucose, substantial gain in potential and increase in current is observed in presence of glucose. This testifies that the immobilized GOx is still active after immobilization and efficiently converts glucose.

Fig. 5B illustrates a comparison between the electrochemical response of Au/ATS/GOx and Au/ATS/PDA/GOx electrodes in presence of 5 mM glucose. It can be observed that compared to the response of Au/ATS/GOx, glucose oxidation at Au/ATS/PDA/GOx starts 461 mV earlier. This difference can only be attributed to presence of PDA in Au/ATS/PDA/GOx electrode, which facilitates the oxidation of glucose. The recorded starting potential of glucose oxidation with Au/ATS/PDA/GOx electrode is better than most of reported values using various GOx-mediator electrodes [4–14]. Also, if compared to Au/ATS/GOx, the current due to glucose oxidation at Au/ATS/PDA/GOx is about 5-times higher, thus relatively substantial keeping in mind that only one layer is deposited. The shift in onset potential towards negative values as well as the significant current response due to glucose oxidation suggests that Au/ATS/PDA/GOx efficiently mediates the catalytic oxidation of glucose. Although it is not yet clear how PDA is linked to GOx, these results demonstrate that both entities PDA and FAD (flavin adenine dinucleotide) of GOx, where the glucose is electrooxidized into gluco-1,5-lactone to generate electrons, are close enough to communicate and yield a facilitated oxidation. Acceleration of rate of the electron transfer by PDA has also been observed elsewhere [34,35]. On the other hand, Au/ATS/PDA without presence of GOx shows an earlier onset potential probably due to the oxidation of PDA because the LSV obtained without presence of glucose is very close to the LSV obtained in presence of 5 mM glucose (Fig. 5B). However, in terms of current, lower values are recorded if compared to the electrode containing the GOx enzyme. This testifies of the importance of both the enzyme GOx and the electron mediator PDA in the constructed bioanode in the efficient conversion of glucose. On the other hand, comparison Au/ATS/PDA in absence of glucose seems to have an earlier onset potential if compared to Au/ATS/PDA/GOx under the same condition (Fig. 5A and B). The later can be related to : i) dissolution of part of the adsorbed PDA on Au/ATS/PDA during the adsorption process of GOx to form Au/ATS/PDA/GOx and/or, ii) presence of GOx in Au/ATS/PDA/GOx renders the oxidation of PDA less facile due to the steric effects induced by GOx. In other words, GOx has a larger volume than PDA, thus if the adsorbed GOx is in direct contact with the electrode surface, it will restrict or prevent PDA to be efficiently oxidized.

In order to clarify how PDA influences the oxidation of glucose, further studies were performed by controlling the deposition time of PDA in the film. Fig. 5C illustrates the response to 5 mM glucose of Au/ATS/PDA/GOx prepared as previously mentioned but by changing the adsorption time of PDA. The variation of starting potential and current intensity of glucose oxidation versus deposition time of PDA is depicted in Fig. 5D. It will be noted that the more deposition time of PDA increases, the more the starting potential of glucose oxidation shifts to lower potentials and the current intensity increases. Similar observations have been noticed regarding the shift in potential of the oxygen reduction reaction with *o*-phenylenediamine (as redox mediator) for laccase enzyme [36]. This suggests that presence of high amount of PDA in the film boosts the catalysis of glucose oxidation. However, it is worth noting that no further improvements in terms of potential and current intensity were recorded for longer adsorption periods, suggesting saturation of the adsorbed layer with PDA. The shift of the onset potential of the enzyme electrode as more PDA is adsorbed suggests that the surface of the electrode is experiencing a different microenvironment from that without presence of PDA. The direction and magnitudes of the shift in potential are consistent with enhanced stabilization of the PDA species by electrostatic interactions [37]. Furthermore, because the potential is shifting towards less positive potentials as the amount of PDA increases, this may suggest that the interior of the film is experiencing an alkaline microenvironment. The latter is maybe the result of binding of PDA within the film to create an alkaline like microenvironment. Finally, it is worth mentioning that once the electrode is fully prepared,

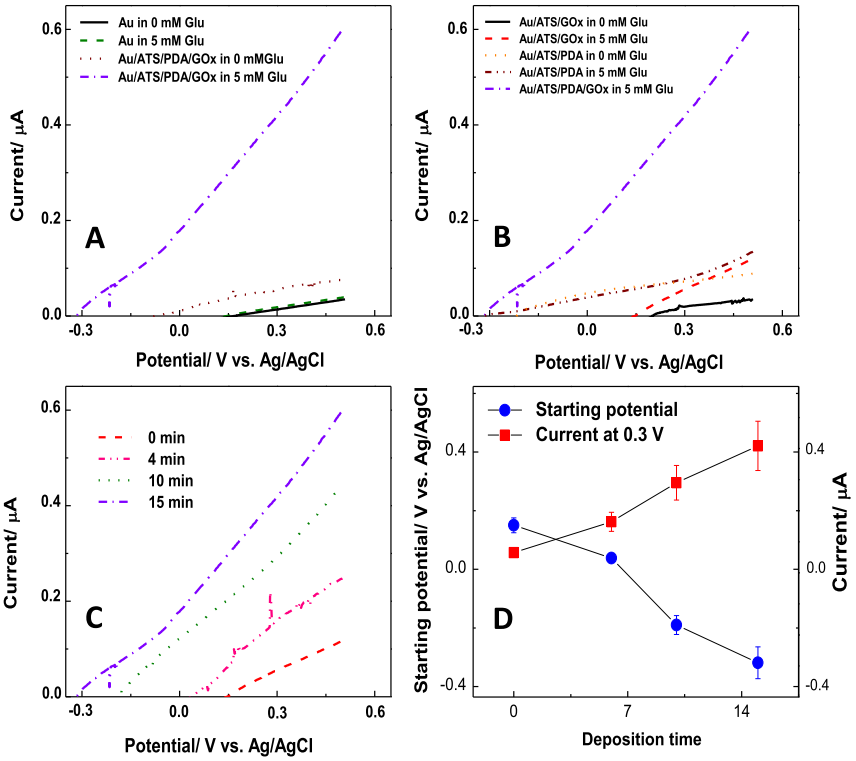

Fig. 5. (A) Comparison between the LSVs of unmodified Au in 5 mM glucose and Au/ATS/PDA/GOx without and with 5 mM glucose. The LSV of unmodified Au without 5 mM glucose is similar to the one shown in (A). (B) Comparison between the linear sweep voltammogram of Au/ATS/GOx and Au/ATS/PDA/GOx modified electrodes in 5 mM glucose showing the importance of presence of PDA in the film. Also is shown Au/ATS/PDA in 0 and 5 mM glucose. (C) LSVs of Au/ATS/PDA/GOx with different adsorption times of PDA tested in presence of 5 mM glucose to record the catalytic oxidation of glucose. (D) Relationship between starting potential and current intensity of glucose oxidation at Au/ATS/PDA/GOx electrode with deposition time of PDA. Test in phosphate buffer solution pH 7.4. Scan rate 20 mV s^{-1}.

rinsed and dried according to the procedure reported in Section 2.3, our observations depict that the Au modified electrode can no longer be modified in the electrochemical cell. In other words, if Au/ATS/GOx was prepared then transferred to the electrochemical cell containing dissolved PDA, the electrochemical response obtained under these conditions is similar to that of Au/ATS/GOx without presence of PDA. This suggests that PDA has absolutely no influence on the Au/ATS/GOx when dissolved in the electrochemical cell, meaning that PDA can not be adsorbed in the electrochemical cell to boost the electron transfer in Au/ATS/GOx and give better electrochemical response. Two parameters may contribute in yielding such a result. First, because the employed electrolyte in the electrochemical cell contains anions and cations, hence they may be the first species to be adsorbed on the electrode and neutralize the functionalized electrode, hence prevent further adsorption. Second, polarization of the electrode (negative then positive potentials) may neutralize the functionalized electrode leading to no further adsorption on the modified electrode. In conclusion, the use of ultrapure water in the modification process of the electrode plays an important role. Because PDA, GOx are dissolved in ultrapure water, hence they are the only species available in solution and thus the one that will be adsorbed on the electrode.

As shown in Fig. 5, the response of the GOx electrode towards glucose does not follow the general path of enzymatic reactions where the response current tends to a limiting plateau at higher potentials. The reason for this may have to do with the following: one hypothesis is that PDA is responsible for the early electrochemical response as verified in Fig. 5B, which reaches a somewhat limiting current based on the adsorption rate of the immobilized mediator. At higher potentials, GOx interfaced with the electrode (which has a higher midpoint potential) contribute mostly to electron transfer. The gradual rise in anodic current suggests that GOx direct electron transfer is a process with a slow interfacial rate of electron transfer.

As illustrated in Fig. 5, oxidation of glucose at Au/ATS/PDA/GOx electrode is quite interesting in terms of starting potential and current efficiency. However, it is observed that when the enzyme electrode is cycled for several times, it loses performance after few cycles, indicating that GOx and PDA are not well stabilized in the film. In order to boost the stability, a last layer of polystyrene sulfonate (PSS) is deposited onto the film by immersing Au/ATS/PDA/GOx electrode in 0.5 mM acetate buffer solution (1 M $CH_3COOLi + CH_3COOH$, pH 5–6) containing 35 mg PSS for at least 15 min. The latter increases the life time of the enzyme electrode because PSS, a negatively charged polyelectrolyte would probably be linked electrostatically to the remaining available positive charged amine groups of ATS [20,21]. This leads to better encapsulation of GOx and PDA within the polyelectrolytes film. As a result, the response of Au/ATS/PDA/GOx/PSS to glucose is quite stable and no deterioration occurs as shown in Fig. 6A. Amperometry also displays that even at polarization of 0.2 V versus Ag/AgCl (Fig. 6A), Au/ATS/PDA/GOx/PSS electrode shows relatively a significant current response in comparison to background current before addition of glucose. Under these conditions, a sensitivity of 51 nA mM^{-1} mm^{-2} is recorded for the first injection. This value is higher than many of the reported GOx enzymes electrodes with self-assembled layers [23,38,39]. Afterward, the sensitivity decreases continuously due either to O_2 depletion in the testing solution or to a slower enzyme kinetics at higher glucose concentrations. Fig. 6A also shows that Au/ATS/PDA/GOx/PSS electrode responds faster to glucose with an average response time of 3 s. The latter was expected since the deposited film is very thin

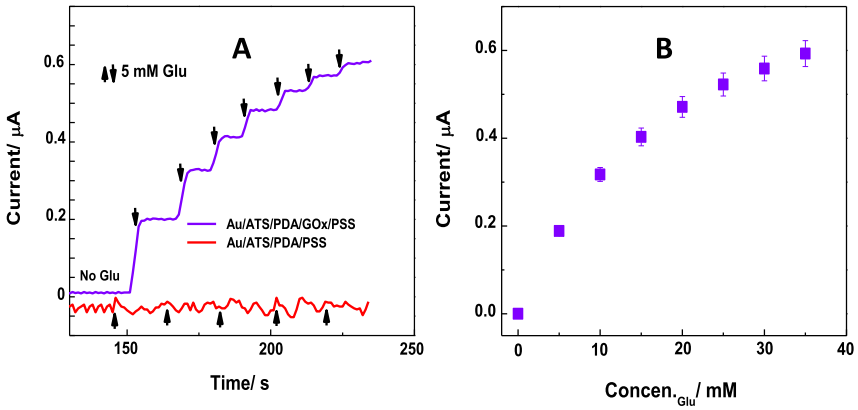

Fig. 6. (A) Typical example of the amperometric response to several additions of 5 mM glucose to Au/ATS/PDA/GOx/PSS electrode polarized at 0.2 V versus Ag/AgCl. Also is shown the response of Au/ATS/PDA/PSS upon addition of several 5 mM glucose for comparison. (B) Relationship between the current response and the glucose concentration taken from (A). Test in phosphate buffer solution pH 7.4 under constant hydrodynamic stirring.

and porous, thus allows a fast diffusion of the glucose molecules throughout the film to be oxidized at the GOx active sites. By comparison, Fig. 6A shows that Au/ATS/PDA/PSS has practically no response to several additions of glucose. The small change in current is due to the noise induced by the injection of glucose and convection phenomena. This means that without the presence of GOx enzyme in the film, no particular catalysis of glucose occurs.

Fig. 6B displays how the current response to glucose varies as a function of the glucose concentration. A linear relationship can be observed in the range 0–10 mM. Above 10 mM, the response is no longer linear and saturates at higher concentrations. The latter might be related to the enzyme kinetics and/or with oxygen depletion from the testing buffer solution.

3.3. Estimation of the surface coverage of Au/ATS/PDA/GOx/PSS electrodes by enzymes molecules

The surface coverage of Au/ATS/PDA/GOx/PSS electrodes by enzyme molecules can be estimated from the electrochemical response of Au/ATS/PDA/GOx/PSS towards glucose oxidation, assuming that all the deposited GOx molecules are active. We know that the specific activity of the glucose oxidase (GOx) is 211 units mg^{-1}. This implies that 1 mg of GOx converts 211×10^{-6} mol of glucose per minute. We will assume that the GOx that is attached to the electrode has the same specific activity as the GOx that is freely suspended in solution. The GOx that is used (derived from *A. Niger*) has a molecular weight of 154×10^3 g mol^{-1} and a diffusion coefficient of 5.02×10^{-11} m^2 s^{-1} at 20 °C in water [40]. Using the Stokes–Einstein equation:

$$D = kT/6\pi\eta a \quad (2)$$

where k is Boltzmann's constant, T is the temperature [K], η is the absolute viscosity [Pa s] and a the hydrodynamic radius of the diffusing species [m], we find a hydrodynamic radius of 4.27 nm for a GOx molecule. Assuming that GOx molecules are roughly spherical, they have a footprint equal to their projected area πa^2 once they are adsorbed on the electrode. For every mole of glucose that is converted, 2 mol of electrons are produced following reaction (3), which will be collected by the Au electrode. From the Lineweaver–Burk analysis, we learned that the maximum current due to the absorbed GOx equals 0.93 μA on an Au electrode with a diameter of 1 mm. In order to produce a current of 0.93 μA, we need 1.37×10^{-6} mg enzyme, which corresponds to 5.36×10^9 molecules of GOx. As each GOx molecules has a footprint of 5.73×10^{-17} m^2, this corresponds to an area of 0.3 mm^2. Assuming that the GOx molecules are randomly close-packed in 2D, which has a packing fraction of 54%, these molecules would occupy a footprint of 0.55 mm^2. However, as the current was measured on the Au electrode with a diameter of 1 mm, the available surface area is 0.78 mm^2. Hence, the maximum current of 0.93 μA can be obtained by a monolayer of GOx molecules with a density equal to 70% of a random close packing.

$$\beta - D - Glucose \xrightarrow{GOx} \delta - glucono - 1,5 - lactone + 2H^+ + 2e^- \quad (3)$$

3.4. Evaluation of Au/ATS/PDA/GOx/PSS as a bioanode for glucose/O_2 BFCs

For the efficient operation of an enzyme-based BFC, a number of conditions must be satisfied. Among the important ones is that redox potential of the bioanode must be as negative as possible to give the maximum potential difference between the bioanode and biocathode. In this respect, Au/ATS/PDA/GOx/PSS electrode showed a substantial gain in potential as previously shown in Fig. 5B. In addition, significant current responses to glucose have also been observed in Figs. 5 and 6. These two attributes designate Au/ATS/PDA/GOx/PSS electrode as a relevant bioanode for BFCs. The Au/ATS/PDA/GOx/PSS bioanode was connected to a clean Pt electrode that is served as a cathode for dioxygen reduction. The two electrodes were connected via two multimeters, one for potential recording and the other for current recording, and immersed in 5 mL phosphate buffer solution pH 7.4 containing 10 mM glucose. The voltage and current were varied using a 1 MΩ potentiometer. Fig. 7A shows the change in power density versus cell voltage and current density versus cell voltage of an Au/ATS/PDA/GOx/PSS bioanode and a Pt cathode. As can be seen, the power density delivered by Au/ATS/PDA/GOx/PSS bioanode reaches 0.25 μW mm^{-2} at potential of 0.76 V. This power density compares well with most of the recently reported glucose bioanodes based thin films [22]. By comparison Au/ATS/PDA/GOx/PSS in absence of glucose does deliver some voltage probably due to difference in potential between Au anode and Pt cathode, but practically no current (Fig. 7A). This demonstrates that the power output is mainly delivered by the catalytic oxidation of glucose that generates electrons which in turn travel through the external circuit to reach the cathode and reduce O_2. By comparison, Au/ATS/PDA/PSS without or with presence of 10 mM glucose also delivers some

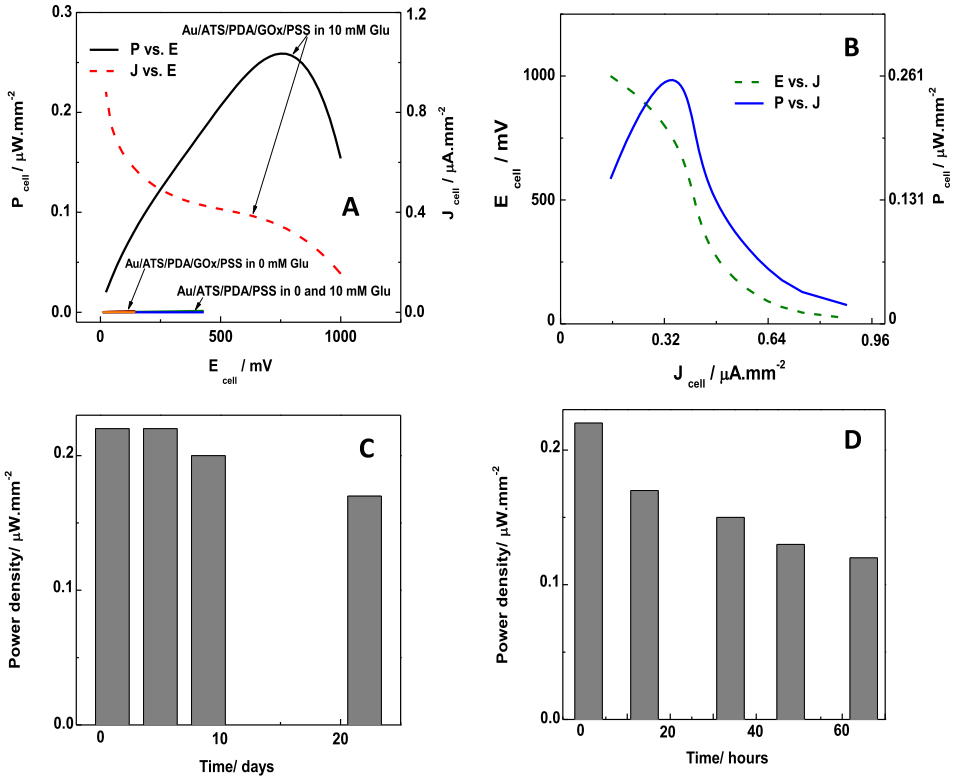

Fig. 7. (A) Typical power density versus cell voltage and current density versus cell voltage of Au/ATS/PDA/GOx/PSS electrode in phosphate buffer solution pH 7.4 containing 10 mM glucose against Pt electrode as a cathode. Also is shown Au/ATS/PDA/GOx/PSS in absence of glucose and Au/ATS/PDA/PSS in presence and absence of 10 mM glucose for comparison. (B) Cell voltage versus current density and power density versus current density for Au/ATS/PDA/GOx/PSS bioanode against Pt cathode. (C) Stability of Au/ATS/PDA/GOx/PSS electrode bioanode over the course of 3 weeks tested with 10 mM glucose. (D) Stability of Au/ATS/PDA/GOx/PSS electrode bioanode over the course of almost 3 days of continuous operation in 10 mM glucose. The electrodes were stored in the fridge at 4 °C.

voltage due to the reason mentioned above, but practically no current (Fig. 7A). The elevated power output recorded with Au/ATS/PDA/GOx/PSS in presence of glucose is due: i) to the low onset potential of glucose oxidation and, ii) to the relatively elevated current response of glucose. In turn, presence of PDA plays an important role in this as previously discussed. By comparison, the estimated power density delivered by Au/ATS/GOx/PSS (without presence of the electron mediator PDA) is only about 0.017 µW mm^{-2}. Finally, it is worth noting that self-assembled monolayers generally form very thin films, thus the delivered power is relatively low if compared to other deposition means like for example encapsulation in polymers/sol gels. However, the power density delivered by the present electrodes maybe boosted if coupled to other deposition processes. In other words, if the PDA can be incorporated successfully with the enzyme in a thick film, the delivered power may significantly be increased.

3.5. Stability

The other condition to satisfy for an efficient operation of an enzyme-based BFC is the stability. The stability of the prepared Au/ATS/PDA/GOx/PSS bioanode was evaluated in phosphate buffer solution pH 7.4 containing 10 mM glucose for a period of 3 weeks. The bioanode was stored in the fridge at 4 °C and tested at regular intervals as shown in Fig. 7C. It will be noted that during this period, the power density of the Au/ATS/PDA/GOx/PSS bioanode decreases only by 19%. This demonstrates that the immobilized GOx enzyme with PDA is well stabilized on the Au electrode. The presence of PSS outer layer plays a very important role in the stabilization process by preventing GOx and PDA from leaking out of the deposited film. On the other hand, when the electrode operated continuously for almost 3 days, it loses about 42% of the initial power (Fig. 7D). The latter compares well with glucose bioanodes subject to continuous operations reported in literature [4–14]. The decrease in power output during continuous operation may simply due to loss in enzyme, mediator or both from the deposited film.

4. Conclusions

In summary, we have demonstrated that Au/ATS/PDA/GOx/PSS constructed via sequential chemical adsorption is viable as a bioanode for glucose/O_2 BFCs for three reasons: i) Au/ATS/PDA/GOx/PSS showed low starting potential for glucose oxidation, ii) Au/ATS/PDA/GOx/PSS displayed relatively high current responses to glucose and, iii) the power output density of Au/ATS/PDA/GOx/PSS is relatively substantial for thin film and stable over time due to the presence of PSS outer layer. Such electrodes might be of interests as bioanodes for *in vitro* and *in vivo* studies. Future work will focus on further characterizations of the enzymes film to figure out the details of the physicochemical interactions within the deposited film. Optimization of the film characteristics and stability, then testing of the bioanodes *in vitro* and *in vivo* for eventual use in powering miniaturized electronic devices like implanted sensors transmitters that do not require high powers.

Acknowledgments

The authors would like to thank the University of Groningen (Netherlands) and KU Leuven (Belgium) for their support.

References

[1] S.C. Barton, J. Gallaway, P. Atanassov, Chem. Rev. 104 (2004) 4867–4886.
[2] A. Heller, Acc. Chem. Res. 23 (1990) 128–134.
[3] G.T.R. Palmore, H.H. Kim, J. Electroanal. Chem. 464 (1999) 110–117.
[4] I. Willner, E. Katz, F. Patolsky, A.F. Buckmann, J. Chem. Soc. Perkin Trans. 2 (1998) 1817–1822.
[5] D. Ivnitski, B. Branch, P. Atanassov, C. Apblett, Electrochem. Commun. 8 (2006) 1204–1210.
[6] C.M. Yu, M.J. Yen, L.C. Chen, Biosens. Bioelectron. 25 (2010) 2515–2521.
[7] E. Nazaruk, K. Sadowska, J.F. Biernat, J. Rogalski, G. Ginalska, R. Bilewicz, Anal. Bioanal. Chem. 398 (2010) 1651–1660.
[8] L. Brunel, J. Denele, K. Servat, K.B. Kokoh, C. Jolivalt, C. Innocent, M. Cretin, M. Rolland, S. Tingry, Electrochem. Commun. 9 (2007) 331–336.
[9] F. Barriere, P. Kavanagh, D. Leech, Electrochim. Acta 51 (2006) 5187–5192.
[10] M. Zhou, L. Deng, D. Wen, L. Shang, L. Jin, S. Dong, Biosens. Bioelectron. 24 (2009) 2904–2908.
[11] P. Jenkins, S. Tuurala, A. Vaari, M. Valkiainen, M. Smolander, D. Leech, Bioelectrochemistry 87 (2012) 172–177.
[12] X. Zhao, H. Jia, J. Kim, P. Wang, Biotechnol. Bioeng. 104 (2009) 1068–1074.
[13] X. Li, H. Zhou, P. Yu, L. Su, T. Ohsaka, L. Mao, Electrochem. Commun. 10 (2009) 851–854.
[14] Y. Yan, W. Zheng, L. Su, L. Mao, Adv. Mater. 18 (2006) 2639–2643.
[15] J.G. Vos, R.J. Forster, T.E. Keyes, Interfacial Supramolecular Assemblies, Wiley, England, 2003, p. 90.
[16] R. Dahint, F. Bender, F. Morhard, Anal. Chem. 71 (1999) 3150–3156.
[17] S.E. Creager, J. Clarke, Langmuir 10 (1994) 3675–3683.
[18] M. Yamaura, R.L. Camilo, L.C. Sampaio, M.A. Macedo, M. Nakamura, H.E. Toma, J. Magn. Magn. Mater. 279 (2004) 210–217.
[19] P.K. Jal, S. Patel, B.K. Mishra, Talanta 62 (2004) 1005–1028.
[20] M. Ammam, B. Keita, L. Nadjo, J. Fransaer, Sens. Actuators B 142 (2009) 347–354.
[21] M. Ammam, B. Keita, L. Nadjo, J. Fransaer, Talanta 80 (2010) 2132–2140.
[22] I. Willner, G. Arad, E. Katz, Bioelectrochem. Bioenerg. 44 (1998) 209–214.
[23] I. Willner, V. HelegShabtai, R. Blonder, E. Katz, G.L. Tao, J. Am. Chem. Soc. 118 (1996) 10321–10322.
[24] Y. Sato, F. Mizutani, J. Electroanal. Chem. 438 (1997) 99–104.
[25] M. Ammam, J. Fransaer, Electrochim. Acta 81 (2012) 129–137.
[26] E. Katz, I. Willner, A.B. Kotlyar, J. Electroanal. Chem. 479 (1999) 64–68.
[27] L.D. White, C.P. Tripp, J. Colloid Interface Sci. 232 (2000) 400–407.
[28] Z. Xu, Q. Liu, J.A. Finch, Appl. Surf. Sci. 120 (1997) 269–278.
[29] S. Ramesh, I. Felner, Y. Koltypin, A. Gedanken, J. Mater. Res. 15 (2000) 944–950.
[30] J. Coates, Interpretation of Infrared Spectra, a Practical Approach, in: R.A. Meyers (Ed.), Encyclopedia of Analytical Chemistry, John Wiley & Sons Ltd, Chichester, 2000, pp. 10815–10837.
[31] M. Jackson, H. Mantsch, Crit. Rev. Biochem. Mol. Biol. 30 (1995) 95–120.
[32] J.J. Feng, G. Zhao, J.J. Xu, H.Y. Chen, Anal. Biochem. 342 (2005) 280–286.
[33] A.J. Bard, R. Faulkner, Electrochemical Methods: Fundamentals and Applications, Wiley, New York, 2001.
[34] Y.T. Fanchiang, J.C.K. Heh, E.S. Gould, Inorg. Chem. 17 (1978) 1142–1145.
[35] F. Peter Guengerich, Chem. Res. Toxicol. 3 (1990) 21–26.
[36] B. Palys, A. Bokun, J. Rogalski, Electrochim. Acta 52 (2007) 7075–7082.
[37] J. Hodak, R. Etchenique, E.J. Calvo, K. Singhal, P.N. Bartlett, Langmuir 13 (1997) 2708–2716.
[38] I. Willner, R. Blonder, E. Katz, A. Stocker, A.F. Buckmann, J. Am. Chem. Soc. 118 (1996) 5310–5311.
[39] E. Katz, A. Riklin, V. Heleg-Shabtai, I. Willner, A.F. Buckmann, Anal. Chim. Acta 385 (1999) 45–58.
[40] J. Raba, H.A. Mottola, Crit. Rev. Anal. Chem. 25 (1995) 1–4.